

1 Metagenomic sequencing detects human respiratory and enteric 2 viruses in air samples collected from congregate settings

3 Nicholas R. Minor^{1‡}, Mitchell D. Ramuta^{2‡}, Miranda R. Stauss¹, Olivia E. Harwood², Savannah F.
4 Brakefield², Alexandra Alberts², William C. Vuyk², Max J. Bobholz², Jenna R. Rosinski², Sydney Wolf²,
5 Madelyn Lund², Madison Mussa², Lucas J. Beversdorf³, Matthew T. Aliota⁴, Shelby L. O'Connor^{1,2},
6 David H. O'Connor^{1,2*}

7 ¹ Wisconsin National Primate Research Center, Madison, WI USA

8 ² Department of Pathology and Laboratory Medicine, University of Wisconsin-Madison, Madison, WI,
9 USA

10 ³ City of Milwaukee Health Department Laboratory, Milwaukee, WI

11 ⁴ Department of Veterinary and Biomedical Sciences, University of Minnesota, Twin Cities, Minneapolis,
12 MN, USA

13 ‡These authors contributed equally.

14 * Correspondence can be addressed to:

15 David H. O'Connor

16 dhoconno@wisc.edu

17 555 Science Drive

18 Madison, WI USA 53711

19 Abstract

20 Innovative methods for evaluating virus risk and spread, independent of test-seeking behavior, are
21 needed to improve routine public health surveillance, outbreak response, and pandemic preparedness.
22 Throughout the COVID-19 pandemic, environmental surveillance strategies, including wastewater and
23 air sampling, have been used alongside widespread individual-based SARS-CoV-2 testing programs
24 to provide population-level data. These environmental surveillance strategies have predominantly
25 relied on pathogen-specific detection methods to monitor viruses through space and time. However,
26 this provides a limited picture of the virome present in an environmental sample, leaving us blind to
27 most circulating viruses. In this study, we explore whether pathogen-agnostic deep sequencing can
28 expand the utility of air sampling to detect many human viruses. We show that sequence-independent
29 single-primer amplification sequencing of nucleic acids from air samples can detect common and
30 unexpected human respiratory and enteric viruses, including influenza virus type A and C, respiratory
31 syncytial virus, human coronaviruses, rhinovirus, SARS-CoV-2, rotavirus, mamastrovirus, and astrovi-
32 rus.

33 Introduction

34 As of September 23rd, 2023, over 70 million SARS-CoV-2 diagnostic tests have been performed in the
35 United States¹. Deploying individual testing programs at this scale is extraordinarily expensive and
36 resource-intensive, and has become increasingly unsustainable in most jurisdictions. New strategies
37 are needed for monitoring the spread and evolution of pathogens without relying on this widespread
38 individual testing.

39 Environmental surveillance, be it through wastewater or air, shows promise for meeting this need.
40 Without relying on individual testing, environmental surveillance has already enabled public health
41 officials to rapidly assess infection risk in congregate settings and in communities writ large²⁻⁵. In
42 the COVID-19 pandemic, the majority of environmental sampling for surveillance purposes has been
43 through wastewater. However, air sampling has several advantages that make it complementary or
44 even preferable to wastewater in certain settings. For example, air samplers are portable and intrin-
45 sically hyperlocal; they can be moved between individual rooms, installed into HVAC systems, and
46 deployed densely in more open areas like airport terminals. Additionally, wastewater sampling may
47 be unfeasible in some areas, such as rural areas where wastewater is disposed of in septic systems.

48 Perhaps most importantly, many human viruses transmit predominantly through aerosols or respiratory
49 droplets, which is exactly what air samplers are designed to collect. Air sampling makes it possible
50 to identify a wide variety of aerosolized viruses while they are in the process of potentially spreading
51 between hosts⁶⁻⁹.

52 However, few studies or real-world air sampler deployments have taken advantage of this bioaerosol
53 diversity. Doing so would require the development of virus-agnostic, metagenomic detection meth-
54 ods, which, when combined with air sampling, could expand surveillance to any airborne virus. Early
55 contributions in this area, e.g.¹⁰⁻¹⁴, demonstrate that it is possible to detect human viruses in various
56 settings. However, this detection comes with a variety of technical challenges¹⁵. First, the relative
57 abundance of aerosolized human viruses in the above studies' air samplers was extremely low. For
58 example, Prussin et al. 2019 characterized airborne viral communities in a daycare center's HVAC
59 system over one year¹¹. Over that year, commonly circulating human viruses accounted for less than
60 0.005% of the total genetic material, with the majority of total virus sequences coming from bacte-
61 riophages and plant-associated viruses. A second challenge is defining which portion of each viral
62 genome to use for classification. Bacteria and fungi have universal genetic marker regions (16S and
63 internal transcribed spacer (ITS) ribosomal RNA, respectively) that are used for sequencing and clas-
64 sification. In contrast, there is no single genetic marker shared across the many viruses that could be
65 present in the air. This leaves unbiased amplification of human virus genetic material as the best option
66 for detecting many, potentially underappreciated viruses in the air¹⁶. One especially promising method
67 is sequence-independent single-primer amplification (SISPA)¹⁷, which has been used to detect a wide
68 range of viruses in clinical samples¹⁸.

69 In 2021, we reported on the characterization of SARS-CoV-2 and other respiratory viruses in air sam-
70 ples collected from congregate settings¹⁹. We also used a semi-quantitative PCR assay in that study
71 to detect 40 other pathogens, demonstrating that air samples could be used to monitor the variety of
72 pathogens that may be present in the spaces around us. Here, we use SISPA to detect an even broad-
73 er array of human RNA viruses from air collected in congregate settings. Understanding human viruses
74 in built environments' air may help elucidate illness trends in communities over time. This approach
75 could enhance air sampling as a tool for public health virus surveillance and preparedness against
76 many emerging and re-emerging viruses.

77 Results

78 Study design

79 From July 2021 to December 2022, we deployed active air samplers in several community settings in
80 the Upper Midwestern states of Wisconsin and Minnesota for routine pathogen monitoring. Thermo
81 Fisher AerosolSense Samplers were used to collect air samples from high-traffic areas in sever-
82 al different congregate settings, including a preschool, campus athletic facility, emergency housing
83 facility, brewery taproom, household, and five K-12 schools. Air samples were collected at weekly and
84 twice-weekly intervals as previously described¹⁹. To demonstrate the feasibility of pathogen-agnostic
85 sequencing to detect human viruses captured in air samples in real-world settings, we analyzed a total
86 of 22 air samples across the 10 congregate settings (Table 1). We also processed three air sample filter
87 substrates from unused AerosolSense cartridges, as no-template controls. Viral RNA was extracted
88 from air samples, and complementary DNA (cDNA) was prepared using sequence-independent sin-
89 gle primer amplification (SISPA) for Oxford Nanopore deep sequencing and metagenomic analysis.
90 Sequencing reads were filtered for host and reagent contaminants and mapped to 835 human-as-
91 sociated viral reference sequences from NCBI to look for common circulating RNA and DNA viruses
92 (available on GitHub at https://github.com/dholab/air-metagenomics/blob/main/resources/ncbi_hu-
93 [man_virus_refseq_20221011.masked.fasta](https://github.com/dholab/air-metagenomics/blob/main/resources/ncbi_human_virus_refseq_20221011.masked.fasta)).

94 **Table 1. Human RNA viruses detected in air samples through deep sequencing with the Oxford**
 95 **Nanopore PromethION.**

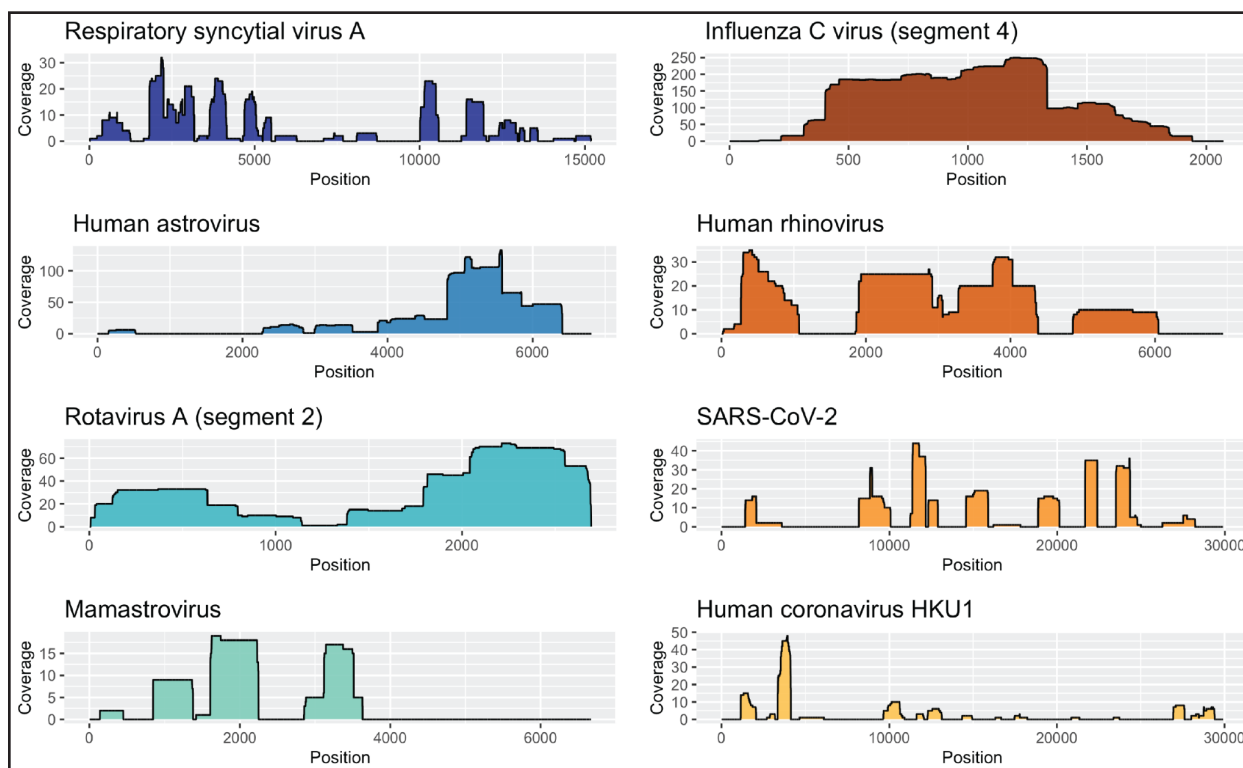
Air sample ID	Location	Start	End	Total number of reads	Pathogen	Number of mapped reads	Percent genome coverage
HC211129	Brewery Taproom	11.22.21	11.29.21	4,113,547	Rotavirus A	276	57.2%
AE000010795B42	Emergency housing shelter	12.21.21	1.7.22	4,898,090	SARS-CoV-2	266	6.5%
AE00001004492C	Campus athletic facility	12.22.21	12.23.21	4,566,986	Respiratory syncytial virus B	182	16.7%
AE0000100A9F46	Preschool	1.5.22	1.19.22	7,037,819	Human astrovirus	70	10.6%
AE0000100A8839	Preschool	1.26.22	2.1.22	4,770,197	Human astrovirus	207	66.3%
					Respiratory syncytial virus A	220	68.9%
					Mamastrovirus	41	26.2%
					Influenza C virus	15	9.2%
AE0000100A8B3C	Preschool	2.1.22	2.8.22	4,022,365	Influenza C virus	1,826	95.0%
					SARS-CoV-2	220	46.7%
					Human rhinovirus	102	68.6%
					Human astrovirus	48	40.2%
					Mamastrovirus	47	36.8%
AE0000100A9532	Preschool	2.23.22	3.1.22	8,252,402	Human coronavirus NL63	921	19.3%
					Influenza C virus	884	38.83%
AE0000100C3430	Elementary school 1	4.11.22	4.19.22	3,205,370	Human coronavirus 229E	8	13.2%
AE0000100CA130	Elementary school 2	3.7.22	3.14.22	4,606,042	Human astrovirus	12	46.2%
					Human Coronavirus NL63	7	11%
					Human coronavirus 229E	4	6%
AE0000100CD638	Elementary school 2	4.4.22	4.18.22	3,945,143	Rotavirus A	50	14.93%
AE0000100CA232	Elementary school 2	4.18.22	5.2.22	3,212,852	Human coronavirus 229E	11	5.8%
AE0000100C7A40	Elementary school 2	5.2.22	5.9.22	4,958,920	NA	NA	NA
AE0000100C702C	Elementary school 2	5.9.22	5.16.22	3,788,598	Rotavirus A	31	37.8%
AE0000100CC536	Elementary school 2	5.16.22	5.23.22	3,920,258	Rotavirus A	105	40.7%
AE0000100CC63D	Elementary school 2	5.23.22	5.31.22	4,836,345	Rotavirus A	40	7.2%
					Simian Agent 10	7	8.9%
AE000010014930	Elementary school 2	11.10.22	11.14.22	8,999,110	Human coronavirus HKU1	5	2.2%
AE000010011724	Elementary school 2	11.22.22	12.1.22	4,946,530	Rotavirus A	3	10.2%
AE00001073172E	Elementary school 3	12.5.22	12.8.22	7560971	Human coronavirus HKU1	113	36.1%
AE00000FEC714A	Middle school	10.31.22	11.3.22	7,421,046	NA	NA	NA
AE00000FEC2245	Middle school	12.5.22	12.8.22	9,380,984	NA	NA	NA
AE0000106DC33E	High school	11.28.22	12.1.22	6,669,497	Influenza A virus	30	10.7%
AE0000100DE93E	Household	4.22.22	4.26.22	6,810,106	Human rhinovirus	17	17.8%
NTC_27269_1	No template control	NA	NA	26,833	NA	NA	NA
NTC2_27269_2	No template control	NA	NA	5,158	NA	NA	NA
NTC_28210	No template control	NA	NA	253,439	NA	NA	NA

96 Percent genome coverage was calculated by summing the total number of basepairs with any amount of read coverage divided by
 97 the total number of basepairs for the given virus target in the RefSeq file. Dates are listed as MM.DD.YY. Abbreviations: NA, not
 98 applicable.

99 Detection of human respiratory and enteric viruses

100 Deep sequencing allowed us to detect human viruses in 19 out of 22 (86%) air samples. No human
 101 viruses were detected in any of the no-template controls. We define a detection of a virus “hit” as two
 102 or more reads mapping to the viral reference sequence in two or more non-overlapping genomic re-

103 gions. By this definition, we detected a total of 13 human RNA viruses in air samples (Table 1). Several
104 of these viruses are associated with frequent and seasonal respiratory illnesses that cause a burden
105 on the healthcare system, including influenza virus type A and C, respiratory syncytial virus subtypes A
106 and B, human coronaviruses (NL63, HKU1, and 229E), rhinovirus, and SARS-CoV-2 (Figure 1). We also
107 detected human viruses associated with enteric disease, including rotavirus, human astrovirus, and
108 mamastrovirus, in ten of the 22 (45%) air samples in this study.

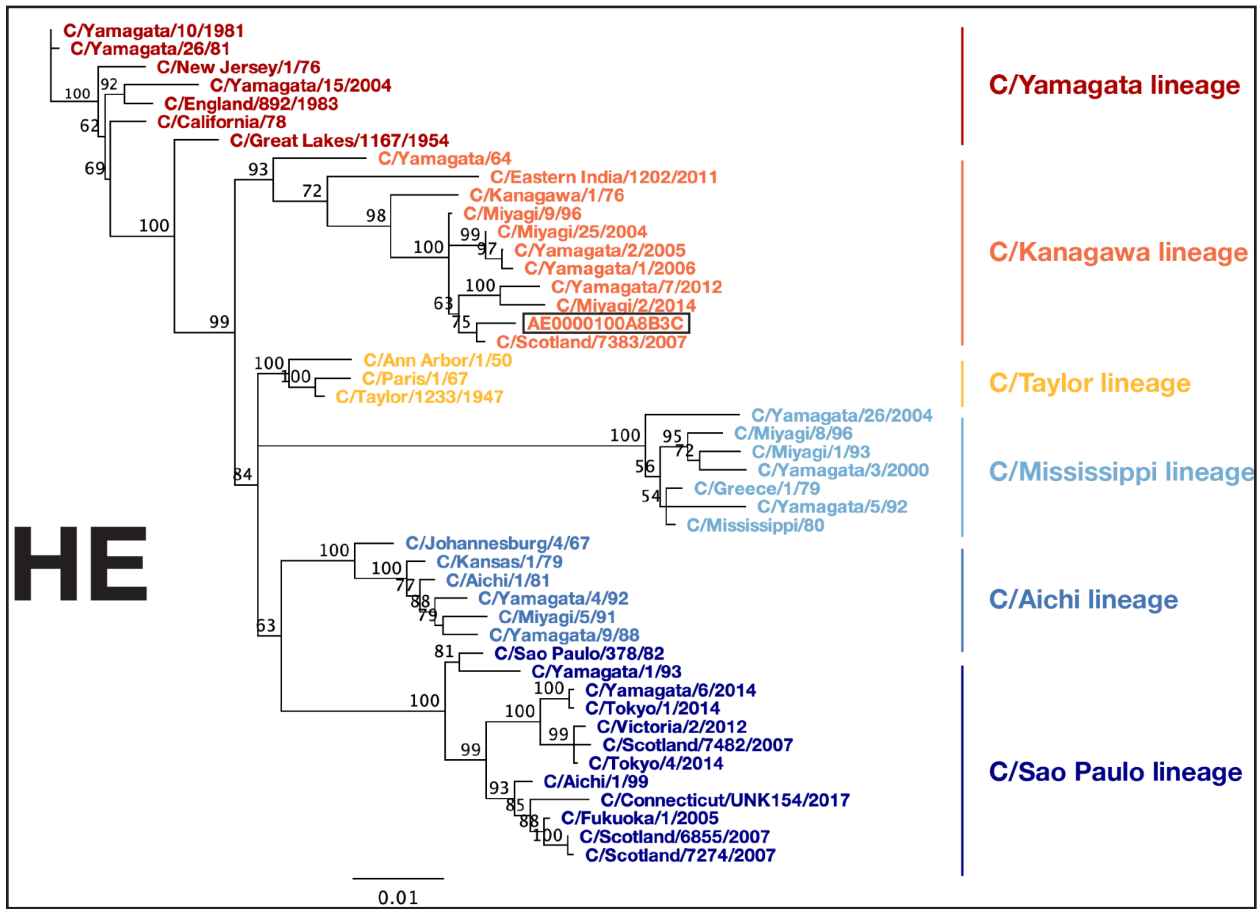


109 **Figure 1. Human respiratory and enteric viruses detected in air samples by SISPA amplification**
110 **and Oxford Nanopore sequencing.** Genome coverage plots showing read depth across eight human
111 RNA viruses detected in air samples. The depth of coverage is shown on the y-axis, and the genome
112 position is shown on the x-axis. The scale of the y-axis varies between plots. Coverage plots were
113 created using ggplot2 (3.4.1) using a custom vR script (4.2.3) in RStudio (2023.03.0+386).
114
115

116 Characterizing influenza C virus lineage in a preschool air sample

117 A preschool air sample from the week of February 1st showed comprehensive coverage of influenza
118 C virus (ICV), with reads mapping to all seven gene segments (supplementary data 1). This included
119 hemagglutinin-esterase (HE), each of the genes encoding proteins for the polymerase complex (PB2,
120 PB1, and P3), nucleoprotein (NP), matrix (M), and nonstructural protein (NS) (supplementary data
121 1). ICV is an understudied respiratory virus, with a total of 2,475 ICV sequences available in NCBI
122 Genbank (taxid:11552) and only 134 ICV sequences submitted from the United States in the 21st cen-
123 tury. To contribute more data on this understudied virus, we used the remaining SISPA-prepared cDNA

124 from the February 1st preschool sample to perform an additional sequencing run with the Oxford
 125 Nanopore GridION. This increased the sample's depth of coverage across the ICV genome compared
 126 to the initial Oxford Nanopore PromethION run, where the flow cell was shared with many samples. We
 127 then used the GridION reads to create consensus sequences for each gene segment, which enabled
 128 us to perform a Tamura-Nei neighbor-joining phylogenetic analysis that compared the February 1st
 129 preschool ICV with 45 other ICV viruses from GenBank (supplementary data 1). Our phylogeny sup-
 130 ported six genetic lineages for the HE gene and two for all other gene segments (Figure 2; supplemen-
 131 tary figure 1). HE grouped with the C/Kanagawa/1/76 lineage. PB2, PB1, M, and NS grouped with the
 132 C/Yamagata/81 lineage. P3 and NP group with C/Mississippi/80 lineage. This particular reassortment
 133 clusters closely with the influenza C virus C/Scotland/7382/2007, which was previously identified by
 134 Smith et al. (Figure 2; supplementary figure 1) ²⁰.



135
 136 **Figure 2. Phylogenetic analysis of influenza C virus hemagglutinin-esterase gene.** Phylogenetic
 137 trees for influenza C virus hemagglutinin-esterase (HE) gene segment. Nucleotide sequences were
 138 aligned using MUSCLE (5.1). The phylogenetic tree was constructed with the Geneious Tree Builder
 139 (2023.0.4) using the Neighbor-joining method and Tamura-Nei model with 100 bootstrapped replicates.
 140 Numbers above the branches indicate the bootstrap values with 100 replicates. ICV strain names are
 141 listed at the end of branches. ICV strains belonging to the C/Sao Paulo lineage are represented in dark
 142 blue, C/Aichi lineage in blue, C/Mississippi lineage in light blue, C/Taylor lineage in yellow, C/Kanagawa

143 lineage in orange, C/Yamagata lineage in red.

144

145 Longitudinal detection of human viruses in a preschool

146 Metagenomic analysis of air samples longitudinally collected from congregate settings can provide
147 insight into changes in the prevalence of pathogens over time. These data could provide public health
148 authorities valuable information to improve routine pathogen surveillance programs and outbreak
149 investigations. To track the prevalence of viral genetic material from ICV and other human viruses in
150 a preschool, we analyzed four air samples that were longitudinally collected from January 5, 2022, to
151 March 1, 2022. ICV was first detected in an air sample collected from January 26th to February 1st,
152 2022. Viral reads in this sample mapped to three out of the seven gene segments including HE, PB2,
153 and NS. Two air samples collected after February 1st, 2022, also contained reads that mapped to
154 several ICV gene segments. ICV genetic material was detected at the highest abundance in air sample
155 AE0000100A8B3C collected from February 1st to the 8th, with reads mapping to all seven gene seg-
156 ments as described above (Table 1; supplementary data 1). Viral reads mapping to five of the seven
157 gene segments, including PB2, PB1, P3, HE, and NP, were detected in an air sample collected from
158 February 23rd to March 1st.

159 Detection of SARS-CoV-2 in RT-PCR-positive air samples

160 To explore whether metagenomic sequencing can detect a human virus that is known to be present
161 in an air sample, we sequenced air samples with known SARS-CoV-2 status. Each AerosolSense
162 cartridge comes with two filter substrates. One filter substrate from each air sample was tested by
163 reverse transcription PCR (RT-PCR) to determine its SARS-CoV-2 status. The other substrate was
164 eluted in 500ul of PBS and stored at -80°C until it was processed for sequencing. Several different RT-
165 PCR assays were used on samples included in this study, depending on when and where they were
166 collected, as previously described¹⁹. Cut-off values used for determining if an air sample was positive,
167 inconclusive, or negative for SARS-CoV-2 are described in the methods section.

168 SISPA sequencing was able to detect SARS-CoV-2 reads in two out of 15 (13.3%) air cartridges that
169 were positive for SARS-CoV-2 by the more sensitive RT-PCR assays (Table 1; supplementary data
170 1). The percent of genome coverage varied between the two samples (6.5% and 46.7%). No SARS-
171 CoV-2 reads were observed in any of the samples that were negative or inconclusive for SARS-CoV-2
172 by RT-PCR testing or with no template controls (supplementary data 1). An inconclusive result was

173 defined as a sample with only amplification in one of the PCR targets. These data suggest that, unsur-
174 prisingly, SISPA sequencing is not as sensitive as RT-PCR for detecting viral genomic material cap-
175 tured in the air samples.

176 Discussion

177 In this study, we used air samples and metagenomic sequencing to detect human RNA viruses in a
178 variety of congregate settings. Specifically, our results show that active air sampling, SISPA library
179 preparation, long-read Oxford Nanopore sequencing, and metagenomic bioinformatics can be used
180 to detect both common and lesser-known human viruses. Because air samplers collect bioaerosols
181 produced when infected individuals breathe, sneeze, cough, or talk, the majority of detected viruses
182 were respiratory. However, we also detected enteric viruses that are transmitted through the fecal-oral
183 route^{21,22}. Several studies have previously used air sampling to detect enteric viruses in congregate
184 settings, including a daycare, a wastewater treatment facility, and a hospital^{11,14,23}. The detection of
185 respiratory viruses in wastewater, and enteric viruses in air samples, creates future opportunities for
186 integration of clinical, wastewater, and air sampler data from the same geographical location to obtain
187 a more comprehensive understanding of viral spread within communities.

188 The most unexpected virus we detected was Influenza C Virus (ICV) in a preschool. SISPA and Oxford
189 Nanopore sequencing allowed us to classify the viral lineages of all seven gene segments of ICV. ICV
190 is a lesser-studied influenza virus that is often excluded from routine respiratory pathogen surveillance
191 programs, which highlights one important limitation of virus-specific surveillance. Despite previous
192 studies having shown a high seroprevalence of ICV in children increasing in age, it suggests that this
193 is a common yet under-ascertained cause of respiratory illness²⁴⁻²⁶, with an epidemiology that remains
194 poorly known^{26,27}. Our ICV results highlight the potential of using air sample networks to detect virus-
195 es that previously had limited awareness. ICV was historically very difficult to detect with cell culture
196 techniques because it causes weak cytopathic effects²⁴, which may lead to an underestimation of ICV
197 prevalence. It will be interesting to see how much more often viruses like ICV are detected as virus-ag-
198 nostic environmental surveillance becomes more prevalent.

199 A potential strength of regular air sample collection, processing, and analysis is characterizing out-
200 breaks longitudinally. For example, we detected the same ICV in the same preschool at four instances,

201 with viral read count rising and falling through time. One possible explanation for this pattern is that it
202 reflects airborne viral RNA load rising and falling over the course of the source infection(s), though we
203 do not have the data to assess host viral load itself. We detect a similar pattern in longitudinal pre-
204 school air sampling for astrovirus, which showed an increase and trailing off of sequencing reads be-
205 tween samples. These results suggest that air sampling can be used to characterize outbreaks in real
206 time. In extended outbreaks, it could also be used to provide early sequencing results, which could
207 then be used to design primers for more sensitive amplification of viruses in the air.

208 All said, we caution that our study does not include a baseline clinical knowledge of all viruses that
209 were present in the settings we sampled. More study will be needed to understand the relationship
210 between air-sampler-derived read counts and airborne viral loads, to determine when a viral load is
211 too low to be detected by our methods, and to rigorously assess the sensitivity and specificity of this
212 approach to pathogen monitoring. However, our SARS-CoV-2 detection results suggest that improving
213 sensitivity may be the best place to start optimizations: while we never detected SARS-CoV-2 in the
214 absence of known infections (no false positives), we failed to detect it in 85% of the cases where an
215 air sample tested positive by a more sensitive qPCR assay.

216 Improvements in bioaerosol collection, nucleic acid library preparation, sequencing technology, and
217 pathogen-agnostic bioinformatics could all significantly improve the detection of human pathogens
218 with air samplers. While SISPA and Oxford Nanopore sequencing enabled us to detect portions of a
219 variety of viral genomes, we inevitably missed additional viruses that were present in the air. Air sam-
220 ples contain high amounts of human, animal, and microbial ribosomal RNA (rRNA), likely associated
221 with airborne microbes and host cells transported on dust particles²⁸. Several studies have shown
222 that rRNA depletion can improve the sensitivity of unbiased sequencing techniques for recovering
223 human RNA viruses from different modalities²⁹, and should be considered for use with air samples.
224 Alternatively, probe-based target capture methods, where nucleic acids eluted from the air cartridge
225 are only retained if they are a reverse complement of a probe sequence³⁰, could be used to enrich
226 viral target sequences. Of note, enriching for a predetermined panel of viruses would make this a
227 multi-pathogen method, not a pathogen-agnostic method²⁹. Even still, the line between multi-patho-
228 gen and pathogen-agnostic is increasingly blurred; commercial kits are available that contain probes
229 for more than 3,000 different viruses, including those with ssRNA, dsRNA, dsDNA, and ssDNA ge-

230 nomes. Truly pathogen-agnostic methods, such as SMART-9N, are also becoming available³¹. These
231 kits have been used with several different sample types to detect common and uncommon viruses in
232 human and animal specimens (nasal swabs and plasma), mosquitoes, and wastewater³²⁻³⁵. Ribosomal
233 RNA depletion and target enrichment both show great promise for enabling air sample networks to
234 screen for pathogens with low abundance in the air.

235 Rapidly evolving sequencing technology could also play a role in improving the efficacy of air sampler
236 networks. Sequencing workflows need to be optimized to be high-throughput, cost effective, and have
237 rapid result turnaround for widespread use with air surveillance programs. In this study we ran two
238 Oxford Nanopore sequencing runs on the PromethION 24. The runs multiplexed 16 and 9 samples
239 and had an output of 85 and 67 Gigabases per flow cell, respectively. The manufacturer estimates
240 a maximal output of 290 Gigabases per flow cell when using newer sequencing kit chemistries³⁶.
241 Improving the sequencing yield to 200 Gigabases could allow for multiplexing up to 32 air samples,
242 while maintaining an average of 6 million Gigabases per air sample. This could make sequencing more
243 cost-effective while maintaining a similar per sample output obtained in this study. Additionally, Oxford
244 Nanopore sequencing enables real-time processing of sequencing data. This could help decrease
245 the turnaround time, as a stream of data will become available as soon as sequencing begins instead
246 of after 72 hours of sequencing has completed. This rapid result turnaround time could be beneficial
247 during outbreak response, when real-time data is essential.

248 The COVID-19 pandemic sparked widespread interest in environmental surveillance strategies for
249 improving pandemic preparedness and outbreak response. While wastewater surveillance has many
250 benefits, air surveillance via active air samplers is more mobile, which makes it easy to quickly deploy
251 air sampling networks in settings of interest such as health clinics, airplanes, ports of entry, public
252 transit, farms, K-12 schools, long-term care facilities, emergency housing facilities, or any other set-
253 ting where people from many places congregate³⁷⁻³⁹. Highlighting this potential application, Mellon et
254 al. recently deployed AerosolSense samplers in an outpatient clinic for patients suspected of mpox
255 infection to look for mpox virus in the air during the 2022 mpox public health emergency of interna-
256 tional concern⁴⁰. Given the portability and flexibility of deployment, air sampling and detection of viral
257 nucleic acids from these samples could become a cornerstone of agile public health responses to viral
258 outbreaks in the near future.

259 Recent advances in metagenomic sequencing technologies have increased efforts to study microbial
260 communities in built environments. This study demonstrates that metagenomic sequencing approach-
261 es paired with air sampling can be used to detect human respiratory and enteric viruses of public
262 health importance in real-world settings. With continual technological improvements and laboratory
263 optimizations, the general framework put forth here could provide a rapid means of monitoring viruses
264 without relying on test-seeking behavior or pathogen-specific assays.

265 **Methods**

266 Ethics Statement

267 Our study does not evaluate the effectiveness of air samplers for diagnosing individuals for COVID-19
268 or other illnesses, nor does it collect samples directly from individuals. Therefore, it does not constitute
269 human subjects research.

270 Air sample collection and processing

271 AerosolSense instruments (Thermo Fisher Scientific) were installed in a variety of indoor congregate
272 settings to collect bioaerosols for pathogen surveillance from December 2021 to December 2023.
273 AerosolSense instruments were placed on flat surfaces 1-1.5 meters off the ground in high-traffic
274 areas of an athletics training facility, preschool, emergency housing facility, brewery taproom, and five
275 K-12 schools in the Upper Midwestern States of Wisconsin and Minnesota. Air samples were collected
276 using AerosolSense cartridges (Thermo Fisher Scientific) according to the manufacturer's instructions.
277 The iOS and Android Askidd mobile app was used to collect air cartridge metadata and upload it to
278 a centralized Labkey database, as previously described in Ramuta et al ¹⁹. After the air samples were
279 removed from the instruments, they were transferred to the lab for further processing. Two air sample
280 substrates were removed from each of the AerosolSense cartridges using sterile forceps to place them
281 in two separate 1.5 mL tubes containing 500 μ L of PBS. The tubes were vortexed for 20 seconds,
282 centrifuged for 30 seconds, and stored at -80°C until RNA extraction and complementary DNA (cDNA)
283 preparation.

284 Air sample total nucleic acid extraction and concentration

285 Total nucleic acids were extracted from air samples using the Maxwell 48 Viral Total Nucleic Acid
286 Purification Kit (Promega) according to the manufacturer's recommendations. Briefly, 300 μ L of air

287 sample eluate was added to a 1.5 μ L tube containing 300 μ L of lysis buffer and 30 μ L of Proteinase K.
288 An unused air cartridge was processed with each Maxwell run to be used as a no-template control.
289 The reaction mix was vortexed for 10 seconds and incubated at 56°C for 10 minutes. Following the
290 incubation, the tubes were centrifuged for 1 minute. Then, 630 μ L of the reaction mix was added to the
291 Maxwell 48 cartridges, which were loaded into a Maxwell 48 instrument and processed with the Viral
292 Total Nucleic Acid program. Nucleic acids were eluted in a final volume of 50 μ L of nuclease-free water.
293 To clean and concentrate the viral RNA, 30 μ L of extracted total nucleic acids were treated with TURBO
294 DNase (Thermo Fisher Scientific) and concentrated to 10 μ L with the RNA Clean & Concentrator-5 kit
295 (Zymo Research) according to the manufacturer's protocols.

296 Air sample sequencing

297 A modified sequence-independent single primer amplification (SISPA) approach previously described
298 by Kafetzopoulou et al. was used to generate cDNA from the air samples^{18,41}. First, 1 μ L of Primer A
299 (Table 2) was added to 4 μ L of concentrated viral RNA and incubated in a thermocycler at 65°C for
300 5 minutes, followed by 4°C for 5 minutes. To perform reverse transcription, 5 μ L of Superscript™ IV
301 (SSIV) First-Strand Synthesis System (Invitrogen) master mix (1 μ L of dNTP (10mM), 1 μ L of nucle-
302 ase-free water, 0.5 μ L of DTT (0.1 M), 2 μ L of 5X RT buffer, and 0.5 μ L of SSIV RT) was added to the
303 reaction mix and incubated in a thermocycler at 42°C for 10 minutes. To perform second-strand cDNA
304 synthesis, 5 μ L of Sequenase Version 2.0 DNA polymerase (Thermo Fisher Scientific) master mix (3.85
305 μ L of nuclease-free water, 1 μ L of 5X Sequenase reaction buffer, and 0.15 μ L of Sequence enzyme)
306 was added to the reaction mix and incubated at 37°C for 8 minutes. After the incubation, 0.45 μ L of
307 the Sequenase dilution buffer and 0.15 μ L of Sequenase were added to the reaction mix and incubat-
308 ed at 37°C for 8 minutes. To amplify the randomly primed cDNA, 5 μ L of the cDNA was added to 45 μ L
309 of the Primer B reaction mix (5 μ L of AccuTaq LA 10x buffer, 2.5 μ L of dNTP (10mM), 1 μ L of DMSO,
310 0.5 μ L of AccuTaq LA DNA polymerase, 35 μ L of nuclease-free water, and 1 μ L of Primer B (Table 2)).
311 The following thermocycler conditions were used to amplify the cDNA: 98°C for 30 seconds, 30 cycles
312 (94°C for 15 seconds, 50°C for 20 seconds, and 68°C for 2 minutes), and 68°C for 10 minutes. The
313 amplified PCR product was purified using a 1:1 ratio of AMPure XP beads (Beckman Coulter) and elut-
314 ed in 25 μ L of nuclease-free water. The purified PCR products were quantified with the Qubit dsDNA
315 high-sensitivity kit (Invitrogen).

317 **Table 2. Sequence independent single primer amplification primers.**

318	Primer Name	Sequence	Concentration
319	Primer A	5'-GTT TCC CAC TGG AGG ATA-(N9)-3'	40 pmol/μL
320	Primer B	5'-GTT TCC CAC TGG AGG ATA -3'	100 pmol/μL

321 Oxford Nanopore sequencing

322 SISPA-prepared cDNA were submitted to the University of Wisconsin-Madison Biotechnology Center
323 for sequencing on the Oxford Nanopore PromethION. Upon arrival, the PCR product concentrations
324 were confirmed with the Qubit dsDNA high-sensitivity kit (Invitrogen). Libraries were prepared with
325 up to 100-200 fmol of cDNA according to the Oxford Nanopore ligation-based sequencing kit SQK-
326 LSK109 and Native Barcoding kit EXP-NBD196. The quality of the finished libraries was assessed
327 using an Agilent TapeStation (Agilent) and quantified again using the Qubit® dsDNA HS Assay Kit
328 (Invitrogen). Samples were pooled and sequenced with an FLO-PRO002 (R9.4.1) flow cell on the
329 Oxford Nanopore PromethION 24 for 72 hours. Data were basecalled using Oxford Nanopore's Guppy
330 software package (6.4.6) with the high accuracy basecalling model (read filtering parameters: minimum
331 length 200 bp, minimum Qscore=9). Air sample AE0000100A8B3C was also sequenced on the Oxford
332 Nanopore GridION to obtain a greater depth of coverage across all seven influenza C virus gene seg-
333 ments. A sequencing library was prepared for AE0000100A8B3C according to the Oxford Nanopore
334 ligation-based sequencing kit SQK-LSK110 instructions. The sample was sequenced with an FLO-
335 MIN106 (R9.4) flow cell on the Oxford Nanopore GridION for 72 hours. Data were basecalled using
336 Oxford Nanopore's Guppy software package (6.4.6) with the high accuracy basecalling model (read
337 filtering parameters: minimum length 20 bp, minimum Qscore=9).

338 **Sequencing analysis**

339 Sequencing data generated from air samples were deposited in the Sequence Read Archive (SRA)
340 under bioproject PRJNA950127. The removal of host reads was requested at the time of SRA submis-
341 sion using the Human Read Removal Tool (HRRT). The sequencing data were analyzed using a custom
342 workflow. To ensure reproducibility and portability, we implemented the workflow in NextFlow and
343 containerized all software dependencies with Docker. All workflow code and replication instructions
344 are publicly available at (<https://github.com/dholab/air-metagenomics>). Briefly, the workflow starts by
345 automatically pulling the study fastq files from SRA, though it has the option of merging locally stored
346 demultiplexed fastq files as well. Then, reads are filtered to a minimum length (200bp) and quality

347 score (Qscore=9), and adapters and barcodes are trimmed from the ends of the reads, all with the
348 reformat.sh script in bbmap (39.01-0). The filtered fastq files for each air sample are then mapped to
349 contaminant FASTA files containing common contaminants with minimap2 (v2.22). Reads that do not
350 map to the contaminant FASTA files are retained and mapped to their sequencing run's negative con-
351 trol reads to further remove contaminants present from library preparation. The cleaned fastq files for
352 each air sample are then mapped to a RefSeq file containing human viruses downloaded from NCBI
353 Virus using minimap2 (v2.22). The human virus reference file contains 835 viral genome sequences
354 and was processed using the bbmask.sh command in bbmap (39.01-0) with default parameters to
355 prevent false-positive mapping to repetitive regions in viral genomes. SAM files for each sample are
356 converted to BAM format, again with reformat.sh. The workflow then completes by generating a pivot
357 table of pathogen "hits," which lists the number of reads supporting each mapped pathogen for each
358 sample. For this study, we then imported the BAM alignments into Geneious Prime (2023.0.4) to
359 inspect the mapping results visually. Genome coverage plots were created for several respiratory and
360 enteric viruses detected in air samples using ggplot2 (3.4.1) with a custom R script (4.2.3) in RStudio
361 (2023.03.0+386).

362 Phylogenetic analysis

363 To compare the influenza C virus detected in the preschool air sample AE0000100A8B3C we down-
364 loaded 45 influenza C virus genome sequences for each of the seven gene segments from Genbank
365 (HE, PB2, PB1, P3, NP, M, and NS). Accession numbers for each segment can be found in supple-
366 mentary data 1. Consensus sequences were generated from AE0000100A8B3C with a minimum cov-
367 erage of 20X. Sections with low coverage were masked with N and trimmed to the reference sequence
368 length. Next, each set of influenza C virus gene segment sequences was aligned using MUSCLE (5.1)
369 implemented in Geneious Prime (2023.0.4) with the PPP algorithm. We then used the Geneious Tree
370 Builder (2023.0.4) to construct a phylogeny for each gene segment using the Neighbor-joining method
371 and Tamura-Nei model with 100 bootstrapped replicates.

372 SARS-CoV-2 RT-PCR

373 Air samples collected between December 2021 and May 2022 were tested for SARS-CoV-2 viral RNA
374 using three different SARS-CoV-2 RT-PCR assays depending on their collection location as previously
375 described¹⁹. Air samples collected after May 2022 were tested for SARS-CoV-2 viral RNA using an RT-

376 PCR protocol as previously described⁴². Briefly, viral RNA was isolated from the air sample substrate
377 using 300 µL of eluate and the Viral Total Nucleic Acid kit for the Maxwell 48 instrument (Promega),
378 following the manufacturer's instructions. RNA was eluted in 50 µL of nuclease-free water. Reverse
379 transcription qPCR was performed using primer and probes from an assay developed by the Centers
380 for Disease Control and Prevention to detect SARS-CoV-2 (N1 and N2 targets). The 20 µL reaction
381 mix contained 5 µL of 4x TaqMan Fast Virus 1-Step Master Mix, 1.5 µL of N1 or N2 primer/probe mix
382 (IDT), 5 µL of sample RNA, and 8.5 µL of nuclease-free water. The RT-PCR amplification was run on a
383 LightCycler 96 at the following conditions: 37°C for 2 minutes, 50°C for 15 minutes, 95°C for 2 min-
384 utes, 50 cycles of 95°C for 3 seconds and 55°C for 30 seconds, and final cool down at 37°C for 30
385 seconds. The data were analyzed in the LightCycler 96 software 1.1 using absolute quantification anal-
386 ysis. Air samples were called positive when N1 and N2 targets both had cycle threshold (Ct) values
387 <40, inconclusive when only one target had Ct <40, and negative if both targets had Ct >40.

388 Data Availability

389 The air sample sequencing data generated in this study have been deposited in the Sequence Read
390 Archive (SRA) under bioproject PRJNA950127. The accession numbers for influenza C virus samples
391 used in the phylogenetic analysis are provided in Supplementary Data 1.

392 **Code Availability**

393 Code to replicate air sample sequencing analysis is available at [https://github.com/dholab/air-metage-](https://github.com/dholab/air-metagenomics)
394 [nomics](https://github.com/dholab/air-metagenomics).

395 **Acknowledgments**

396 This work was made possible by financial support through the National Institutes of Health grant
397 (AAL4371). M.D.R. is supported by the National Institute of Allergy and Infectious Diseases of the
398 National Institutes of Health under Award Number T32AI55397. The author(s) thank the University
399 of Wisconsin Biotechnology Center DNA Sequencing Facility (Research Resource Identifier –
400 RRID:SCR_017759) for providing PromethION sequencing services. We would like to acknowledge Eli
401 O'Connor's work in developing the iOS and Android Askidd mobile app to help streamline air sample
402 metadata collection. We would like to thank all of the participating congregations for their part-
403 nership during this study.

405 Author contributions

406 N.R.M contributed to the formal analysis, investigation, methodology, writing—original draft prepara-
407 tion and writing as well as revision—review and editing. M.D.R contributed to the conceptualiza-
408 tion, data curation, formal analysis, investigation, methodology, project administration, visualization,
409 writing—original draft preparation, writing—review and editing. D.H.O and S.L.O. contributed to the
410 conceptualization, project administration, writing—original draft preparation, and writing—review and
411 editing. M.R.S., O.E.H., A.A., W.C.V., M.J.B., and J.R.R. contributed to data curation, logistics, organi-
412 zation, and writing—review and editing. L.J.B. and M.T.A. contributed to data curation, resources, proj-
413 ect management, and writing—review and editing. S.F.B, S.W., M.L., and M.M. contributed to logistics,
414 organization, and writing—review and editing.

415 References

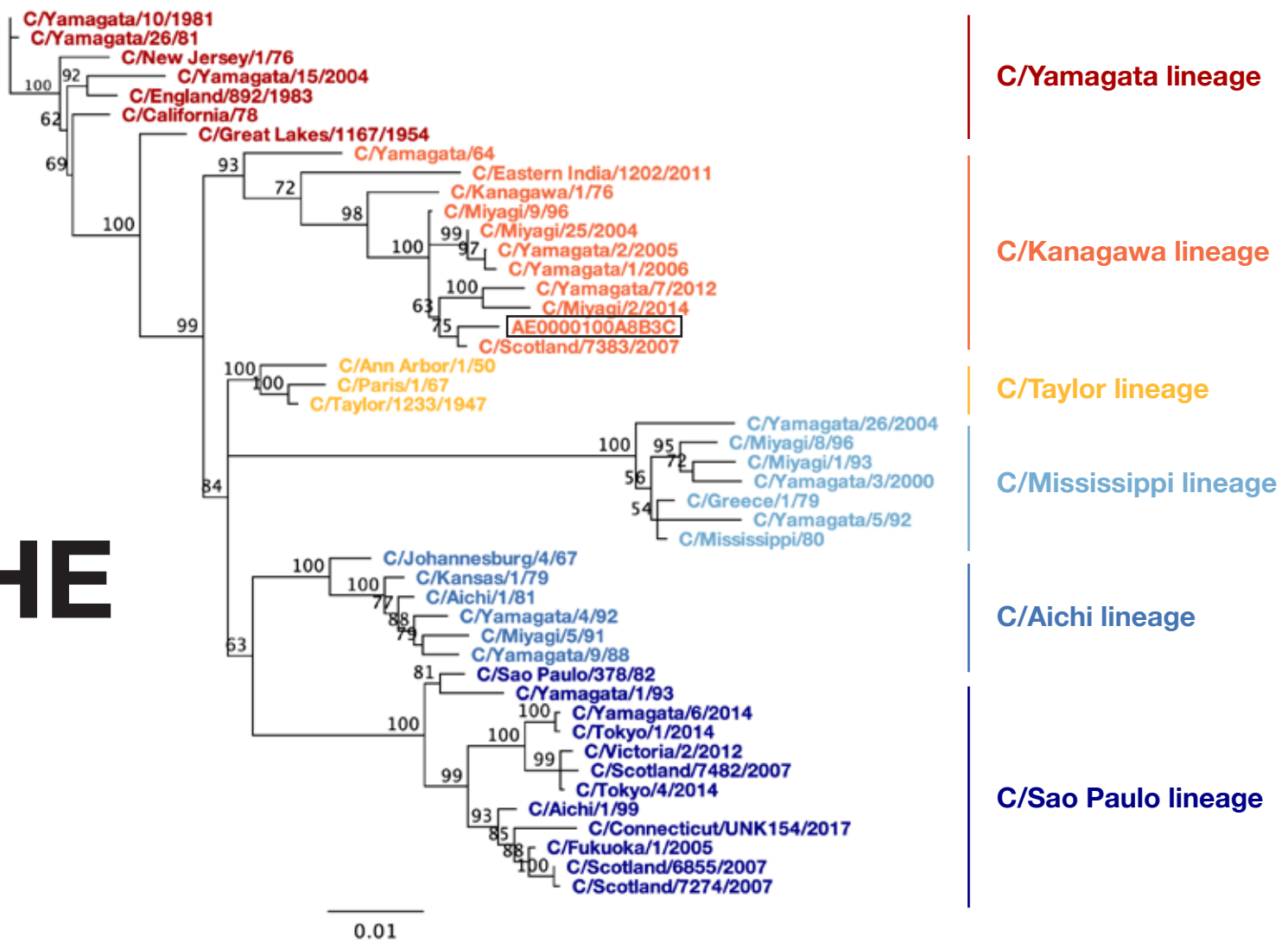
- 416 1. CDC. COVID data tracker. *Centers for Disease Control and Prevention* [https://covid.cdc.gov/](https://covid.cdc.gov/covid-data-tracker/)
417 [covid-data-tracker/](https://covid.cdc.gov/covid-data-tracker/) (2020).
- 418 2. Polo, D. *et al.* Making waves: Wastewater-based epidemiology for COVID-19 - approaches and
419 challenges for surveillance and prediction. *Water Res.* **186**, 116404 (2020).
- 420 3. Kirby, A. E. *et al.* Using Wastewater Surveillance Data to Support the COVID-19 Response -
421 United States, 2020-2021. *MMWR Morb. Mortal. Wkly. Rep.* **70**, 1242–1244 (2021).
- 422 4. Kirby, A. E. *et al.* Notes from the Field: Early Evidence of the SARS-CoV-2 B.1.1.529 (Omicron)
423 Variant in Community Wastewater - United States, November-December 2021. *MMWR Morb. Mortal.*
424 *Wkly. Rep.* **71**, 103–105 (2022).
- 425 5. McClary-Gutierrez, J. S. *et al.* SARS-CoV-2 Wastewater Surveillance for Public Health Action.
426 *Emerg. Infect. Dis.* **27**, 1–8 (2021).
- 427 6. Yang, W., Elankumaran, S. & Marr, L. C. Concentrations and size distributions of airborne influ-
428 enza A viruses measured indoors at a health centre, a day-care centre and on aeroplanes. *J. R. Soc.*
429 *Interface* **8**, 1176–1184 (2011).
- 430 7. Prussin, A. J., 2nd & Marr, L. C. Sources of airborne microorganisms in the built environment.
431 *Microbiome* **3**, 78 (2015).
- 432 8. Wang, C. C. *et al.* Airborne transmission of respiratory viruses. *Science* **373**, (2021).
- 433 9. Myatt, T. A. *et al.* Detection of airborne rhinovirus and its relation to outdoor air supply in office
434 environments. *Am. J. Respir. Crit. Care Med.* **169**, 1187–1190 (2004).

- 435 10. Rosario, K., Fierer, N., Miller, S., Luongo, J. & Breitbart, M. Diversity of DNA and RNA Viruses in
436 Indoor Air As Assessed via Metagenomic Sequencing. *Environ. Sci. Technol.* **52**, 1014–1027 (2018).
- 437 11. Prussin, A. J., 2nd *et al.* Seasonal dynamics of DNA and RNA viral bioaerosol communities in a
438 daycare center. *Microbiome* **7**, 53 (2019).
- 439 12. Be, N. A. *et al.* Metagenomic analysis of the airborne environment in urban spaces. *Microb.*
440 *Ecol.* **69**, 346–355 (2015).
- 441 13. Hall, R. J. *et al.* Metagenomic detection of viruses in aerosol samples from workers in animal
442 slaughterhouses. *PLoS One* **8**, e72226 (2013).
- 443 14. Brisebois, E. *et al.* Human viral pathogens are pervasive in wastewater treatment center aero-
444 sols. *J. Environ. Sci.* **67**, 45–53 (2018).
- 445 15. Prussin, A. J., 2nd, Marr, L. C. & Bibby, K. J. Challenges of studying viral aerosol metagenom-
446 ics and communities in comparison with bacterial and fungal aerosols. *FEMS Microbiol. Lett.* **357**, 1–9
447 (2014).
- 448 16. Prussin, A. J., 2nd *et al.* Viruses in the Built Environment (VIBE) meeting report. *Microbiome* **8**, 1
449 (2020).
- 450 17. Reyes, G. R. & Kim, J. P. Sequence-independent, single-primer amplification (SISPA) of com-
451 plex DNA populations. *Mol. Cell. Probes* **5**, 473–481 (1991).
- 452 18. Kafetzopoulou, L. E. *et al.* Assessment of metagenomic Nanopore and Illumina sequencing for
453 recovering whole genome sequences of chikungunya and dengue viruses directly from clinical sam-
454 ples. *Euro Surveill.* **23**, (2018).
- 455 19. Ramuta, M. D. *et al.* SARS-CoV-2 and other respiratory pathogens are detected in continuous
456 air samples from congregate settings. *Nat. Commun.* **13**, 4717 (2022).
- 457 20. Smith, D. B., Gaunt, E. R., Digard, P., Templeton, K. & Simmonds, P. Detection of influenza C
458 virus but not influenza D virus in Scottish respiratory samples. *J. Clin. Virol.* **74**, 50–53 (2016).
- 459 21. Ghosh, S. *et al.* Enteric viruses replicate in salivary glands and infect through saliva. *Nature*
460 **607**, 345–350 (2022).
- 461 22. Zhuo, R. *et al.* Identification of Enteric Viruses in Oral Swabs from Children with Acute
462 Gastroenteritis. *J. Mol. Diagn.* **20**, 56–62 (2018).
- 463 23. Dennehy, P. H., Nelson, S. M., Crowley, B. A. & Saracen, C. L. Detection of Rotavirus RNA in
464 Hospital Air Samples by Polymerase Chain Reaction (PCR) • 828. *Pediatr. Res.* **43**, 143–143 (1998).

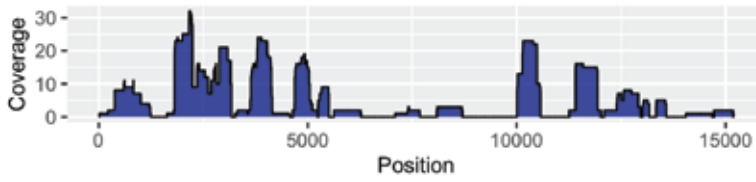
- 465 24. Sederdahl, B. K. & Williams, J. V. Epidemiology and Clinical Characteristics of Influenza C Virus.
466 *Viruses* **12**, (2020).
- 467 25. Atkinson, K. V. *et al.* Influenza C in Lancaster, UK, in the winter of 2014–2015. *Sci. Rep.* **7**,
468 46578 (2017).
- 469 26. Matsuzaki, Y. *et al.* Genetic Lineage and Reassortment of Influenza C Viruses Circulating be-
470 tween 1947 and 2014. *J. Virol.* **90**, 8251–8265 (2016).
- 471 27. Daniels, R. S. *et al.* Molecular Characterization of Influenza C Viruses from Outbreaks in Hong
472 Kong SAR, China. *J. Virol.* **94**, (2020).
- 473 28. Rai, S., Singh, D. K. & Kumar, A. Microbial, environmental and anthropogenic factors influenc-
474 ing the indoor microbiome of the built environment. *J. Basic Microbiol.* **61**, 267–292 (2021).
- 475 29. Fitzpatrick, A. H. *et al.* High Throughput Sequencing for the Detection and Characterization of
476 RNA Viruses. *Front. Microbiol.* **12**, 621719 (2021).
- 477 30. Ballester, L. Y., Luthra, R., Kanagal-Shamanna, R. & Singh, R. R. Advances in clinical next-gen-
478 eration sequencing: target enrichment and sequencing technologies. *Expert Rev. Mol. Diagn.* **16**,
479 357–372 (2016).
- 480 31. Claro, I. M. *et al.* Rapid viral metagenomics using SMART-9N amplification and nanopore se-
481 quencing. *Wellcome Open Res* **6**, 241 (2021).
- 482 32. Terwilliger, A. *et al.* HIV Detection in Wastewater as a Potential Epidemiological Bellwether.
483 (2022) doi:10.2139/ssrn.4257909.
- 484 33. Kim, K. W. *et al.* Respiratory viral co-infections among SARS-CoV-2 cases confirmed by virome
485 capture sequencing. *Sci. Rep.* **11**, 3934 (2021).
- 486 34. Wang, Y. *et al.* SARS-CoV-2 Exposure in Norway Rats (*Rattus norvegicus*) from New York City.
487 *MBio* e0362122 (2023).
- 488 35. Yamaguchi, J. *et al.* 548. Target Enriched NGS Reveals Wide Breadth of Viruses Causing Acute
489 Undifferentiated Fever in Thailand. *Open Forum Infect Dis* **9**, ofac492.601 (2022).
- 490 36. *PromethION 2 Solo Technical Specification*. [https://community.nanoporetech.com/require-](https://community.nanoporetech.com/requirements_documents/promethion-2s-spec.pdf)
491 [ments_documents/promethion-2s-spec.pdf](https://community.nanoporetech.com/requirements_documents/promethion-2s-spec.pdf) (2022).
- 492 37. Anderson, B. D. *et al.* Bioaerosol Sampling in Modern Agriculture: A Novel Approach for
493 Emerging Pathogen Surveillance? *J. Infect. Dis.* **214**, 537–545 (2016).
- 494 38. Bailey, E. S., Choi, J. Y., Zemke, J., Yondon, M. & Gray, G. C. Molecular surveillance of respira-
495 tory viruses with bioaerosol sampling in an airport. *Trop Dis Travel Med Vaccines* **4**, 11 (2018).

- 496 39. Coleman, K. K. *et al.* Bioaerosol Sampling for Respiratory Viruses in Singapore’s Mass Rapid
497 Transit Network. *Sci. Rep.* **8**, 17476 (2018).
- 498 40. Mellon, G. *et al.* Air detection of monkeypox virus in a dedicated outpatient clinic room for
499 monkeypox infection diagnosis. *J. Infect.* **86**, 256–308 (2023).
- 500 41. Moreno, G. K. *et al.* Revealing fine-scale spatiotemporal differences in SARS-CoV-2 introduc-
501 tion and spread. *Nat. Commun.* **11**, 5558 (2020).
- 502 42. Newman, C. M. *et al.* Initial Evaluation of a Mobile SARS-CoV-2 RT-LAMP Testing Strategy. *J.*
503 *Biomol. Tech.* **32**, 137–147 (2021).

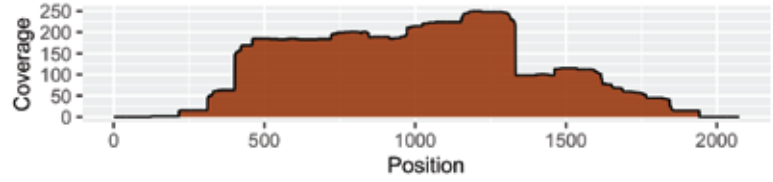
HE



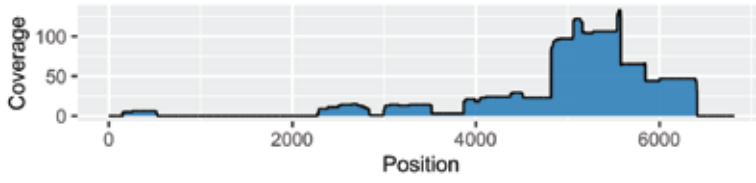
Respiratory syncytial virus A



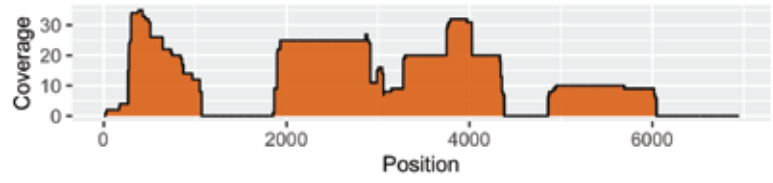
Influenza C virus (segment 4)



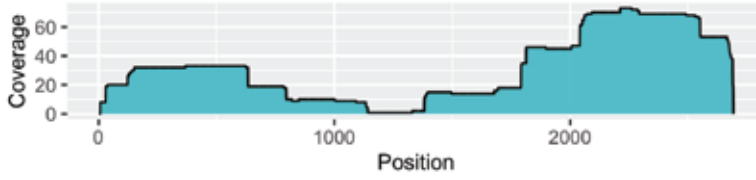
Human astrovirus



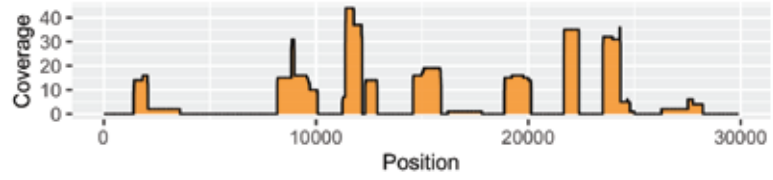
Human rhinovirus



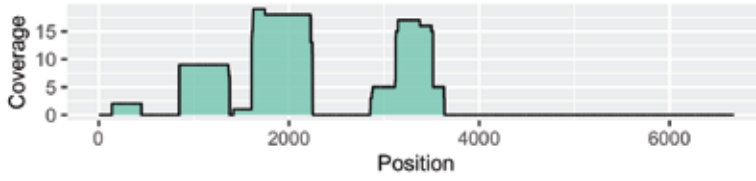
Rotavirus A (segment 2)



SARS-CoV-2



Mamastrovirus



Human coronavirus HKU1

